

**Supporting Information for:**

**“Isotope-Edited FTIR of Alkaline Phosphatase  
Resolves Paradoxical Ligand Binding Properties and  
Suggests a Role for Ground State Destabilization”**

*Logan D. Andrews<sup>a</sup>, Hua Deng<sup>b</sup>, and Daniel Herschlag<sup>a,c,d</sup>*

<sup>a</sup>Department of Chemical and Systems Biology and <sup>c</sup>Department of Biochemistry, Stanford University, Stanford, California 94305. <sup>b</sup>Department of Biochemistry, Albert Einstein College of Medicine, 1300 Morris Park Avenue, Bronx, New York 10461

<sup>d</sup>Corresponding author:

Dept. of Biochemistry, B400

Stanford University

Stanford, CA 94305-5307

650-723-9442 (telephone)

650-723-6783 (fax)

[herschla@stanford.edu](mailto:herschla@stanford.edu)

## AP Catalytic Rate Enhancement and Affinity for the Substrate Transition State

The rate enhancement provided by AP is the ratio of the catalyzed and uncatalyzed phosphate monoester hydrolysis rate constants – the enzyme reacts with the phosphate monoester dianion so for comparison the uncatalyzed rate constant considered must also be for the dianion. Previous measurements of the uncatalyzed phosphate monoester dianion hydrolysis reaction estimated that the first order rate constant is  $2 \times 10^{-20} \text{ s}^{-1}$  for attack by water at 25 °C.<sup>1</sup> Dividing the first-order rate constant by the concentration of water (55 M) yields a second order rate constant of  $3.6 \times 10^{-22} \text{ M}^{-1} \text{ s}^{-1}$ . AP catalyzes this hydrolysis with a second-order rate constant ( $k_{\text{cat}}/K_{\text{M}}$ ) of  $1.2 \times 10^6 \text{ M}^{-1} \text{ s}^{-1}$ , giving a ration that represents the rate enhancement of  $3 \times 10^{27}$ -fold.<sup>2</sup>

Reaction rate constants can be converted to apparent equilibrium constants using Eyring's transition state theory by eq S1 and S2

$$k_{\text{uncat}} = (kT/h)K_{\text{uncat}}^{\ddagger} \quad (\text{S1})$$

$$k_{\text{enzyme}} = (kT/h)K_{\text{enzyme}}^{\ddagger} \quad (\text{S2})$$

where  $k$  is the Boltzmann constant,  $T$  is the absolute temperature, and  $h$  is Planck's constant. The equilibrium constants are defined in Figure S1. These equilibrium constants can be expressed as free energy changes by the standard relationship between free energies and equilibrium constants (eq S3 and S4;  $R$  is the gas constant; assuming a standard state of 1M).

$$\Delta G_{\text{uncat}}^{\ddagger} = -RT \ln(K_{\text{uncat}}^{\ddagger}) \quad (\text{S3})$$

$$\Delta G_{\text{enzyme}}^{\ddagger} = -RT \ln(K_{\text{enzyme}}^{\ddagger}) \quad (\text{S4})$$

The difference between the free energies from eq S3 and S4 gives the energetic stabilization of the reaction transition state by the enzyme. This energetic difference can be expressed as,

$$\Delta \Delta G^{\ddagger} = RT \ln(k_{\text{enzyme}}/k_{\text{uncat}}) \quad (\text{S5})$$

which for a rate enhancement of  $10^{27}$ -fold at room temperature (298 K) corresponds to 37 kcal/mol. This energetic difference is also equivalent to the enzyme's theoretical affinity for the substrate transition state ( $S^\ddagger$ ), which is described by the equilibrium constant  $K_T$  in Figure S1. The following relationships illustrate this equivalence:

$$K_{\text{enzyme}}^\ddagger = K_{\text{uncat}}^\ddagger \times K_T \quad (\text{S6})$$

$$K_{\text{enzyme}}^\ddagger / K_{\text{uncat}}^\ddagger = K_T \quad (\text{S7})$$

$$K_T = k_{\text{enzyme}} / k_{\text{uncat}} = e^{\Delta\Delta G^\ddagger / RT} \quad (\text{S8})$$

Thus, the theoretical affinity of AP for the phosphate monoester dianion transition state is also 37 kcal/mol. The theoretical affinity reflects the binding of the enzyme to the transition state while accompanied by the replacement of water by the active site Ser102 for the enzyme-catalyzed reaction. The energetics of these two processes cannot be separated but correspond to an overall energetic change of 37 kcal/mol upon formation of the enzyme transition state complex.

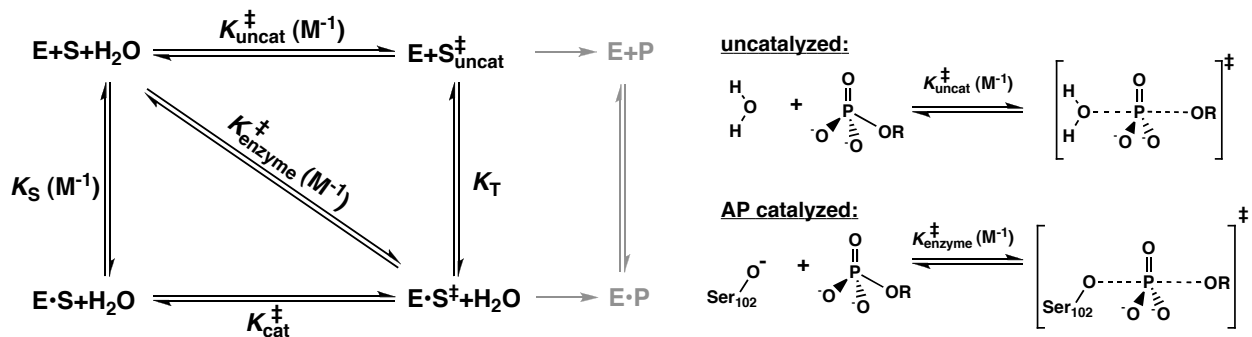
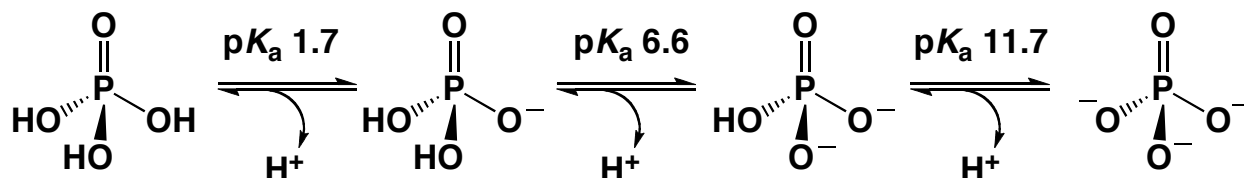


**Figure S1.** General reaction scheme for an enzymatic reaction and the corresponding bimolecular nonenzymatic reaction. From transition state theory, equilibrium constants between ground states and transition states can be related to observed rate constants as described in text. As thermodynamics is pathway independent the ratio of  $K_{\text{enzyme}}^\ddagger$  and  $K_{\text{uncat}}^\ddagger$  is equal to  $K_T$ , the formal equilibrium constant for transition state binding to the enzyme.

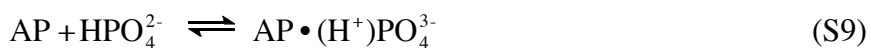
## Evidence from Prior Studies That the P<sub>i</sub> Dianion Does Not Release a Proton to Solution Upon Binding AP

Free inorganic phosphate (P<sub>i</sub>) can exist in several different ionic forms depending on the solution pH (Scheme S1; pK<sub>a</sub>'s reported for 25 °C, 0.5 M ionic strength<sup>3</sup>), and therefore AP could, in principle, bind any or multiple P<sub>i</sub> species from solution.



### Scheme S1

The binding affinity of AP for P<sub>i</sub> measured across pH reveals the number of protons taken up by the complex or released to solution upon association of the preferred solution P<sub>i</sub> species and predominate free AP species at each pH. Previous binding studies show a log linear increase in AP•P<sub>i</sub> affinity as the pH is raised from 4.5 to ~6 (Figure S2A).<sup>4</sup> Over this pH range the P<sub>i</sub> dianion (HPO<sub>4</sub><sup>2-</sup>) becomes more and more populated in solution as the P<sub>i</sub> monoanion (H<sub>2</sub>PO<sub>4</sub><sup>1-</sup>) pK<sub>a</sub> is ~6.6 under these conditions. The log-linear increase in AP binding affinity with a slope of 1 at low pH then suggests that AP has no measurable affinity for H<sub>2</sub>PO<sub>4</sub><sup>1-</sup> or equivalently, that a proton is lost upon binding. The slope of 1 levels to zero with an apparent pK<sub>a</sub> of 6.6, indicating no gain or loss of a proton upon binding and consistent with binding of HPO<sub>4</sub><sup>2-</sup> in the region above 6.6. This model, with HPO<sub>4</sub><sup>2-</sup> binding, is represented in eq S9 and is the simplest model consistent with the data. (So far we consider only the data up to pH 8.)



We next consider an alternative model for P<sub>i</sub> binding in which HPO<sub>4</sub><sup>2-</sup> binds but loses its proton to solution, as illustrated in eq S10. This is the model that we note in the main text is ruled out by prior data.



In the eq S10 model, the binding of HPO<sub>4</sub><sup>2-</sup> occurs with loss of a proton and is thus thermodynamically equivalent to the binding of the free P<sub>i</sub> trianion (PO<sub>4</sub><sup>3-</sup>) from solution. The observed P<sub>i</sub> binding affinity would therefore reflect the available population of PO<sub>4</sub><sup>3-</sup> at any given pH. At pH values below 6.6, *two* protons must be lost to give PO<sub>4</sub><sup>3-</sup>, so that a drop in binding affinity with a slope of 2 (log-linear) is predicted. The experimentally observed slope of 1 at the acidic pH values therefore, provides evidence against this model.

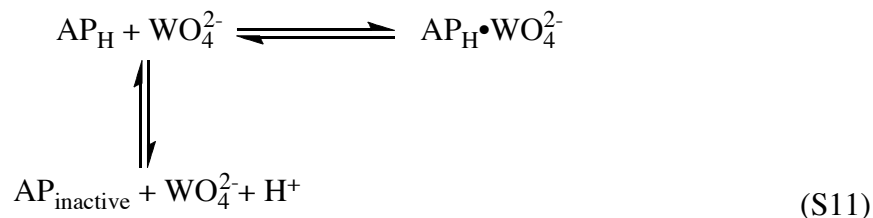
Further, the binding of P<sub>i</sub> levels off at pH values above 6.6, the pK<sub>a</sub> for formation of HPO<sub>4</sub><sup>2-</sup>. If PO<sub>4</sub><sup>3-</sup> bound from solution then an additional proton would need to be lost and binding would continue to increase log-linearly with a slope of 1 above pH 6.6, which is not observed.

Additional support for the model of eq S9 comes from the observation that the observed pK<sub>a</sub> in pH-dependences such as that in Figure S2A give different pK<sub>a</sub>'s for different ligands (or substrates), with the pK<sub>a</sub> mirroring the solution pK<sub>a</sub> of the binding or reacting group<sup>4</sup> – i.e. the observed pK<sub>a</sub> reflects the known pK<sub>a</sub> of the ligand. Nevertheless, complexities from protonation and deprotonation events on the enzyme are possible. The simplest data that rule out such complexities (for data below pH 8) are shown in Figure S2B for binding of tungstate to AP and are described below.

To isolate any potential protonation events associated with AP and not the binding ligand, the pH-dependent binding affinity of a molecule that does not have a pK<sub>a</sub> in the pH region of interest was measured.<sup>4</sup> The AP binding affinity for tungstate, which has a single pK<sub>a</sub> of ~4, was

measured as a function of pH (Figure S2B). The binding is flat from pH 4.5 to 8, indicating that there are no enzymatic protonation or deprotonation events that affect ligand binding across this pH range, and the model of eq S9 is strongly supported whereas that of S10 is ruled out.

The pH-dependence for tungstate binding does reveal a complexity above pH 8, but this complexity also leads to support for the eq S9 model and evidence against the eq S10 model – i.e. formal binding of  $\text{HPO}_4^{2-}$  and not  $\text{PO}_4^{3-}$ . The pH dependence for tungstate binding reveals a log-linear decrease in binding affinity at pH values above 8 with a slope of one, as observed for  $\text{P}_i$  binding (Figure S2A and S2B). Because the observed decrease cannot be associated with a  $\text{p}K_a$  of free tungstate, this decrease must represent a deprotonation event associated with AP itself, with an inactivating  $\text{p}K_a$  of 8. [The  $\text{p}K_a$  is observed in pH dependencies of binding, as in Figure S2, and catalytic activity (see ref. 4; data not shown).] The model for tungstate binding that follows from the above results is described by eq S11.



Given this inactivating  $\text{p}K_a$  of 8, if  $\text{HPO}_4^{2-}$  binds then binding should weaken log-linearly above pH 8, as there are no  $\text{p}K_a$ 's for  $\text{P}_i$  from 6.6 to >11 (Scheme S1). This dependence is observed in Figure S2A. In contrast, if  $\text{PO}_4^{3-}$  were to bind, it would have to lose a proton while AP would need to gain a proton to be in a binding-active state, so that a flat pH-dependence for binding would be predicted. The observed log-linear dependence with slope -1 then provides additional evidence ruling out model of eq S10. In summary, both the pH-dependent  $\text{P}_i$  and tungstate data support the model of eq S9 and rule out that of eq S10. While eq S9 requires that the  $\text{HPO}_4^{2-}$  proton remain part of the bound complex, the pH-dependent data do not reveal where

the proton is within the complex – i.e. if the proton remains on  $P_i$  or gets transferred to AP. An FTIR approach was used to distinguish between these possibilities as described in the main text.

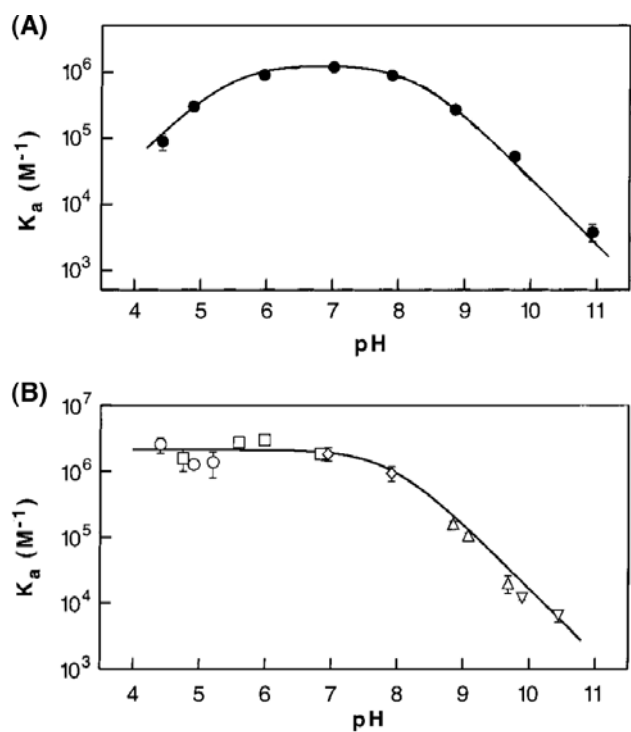


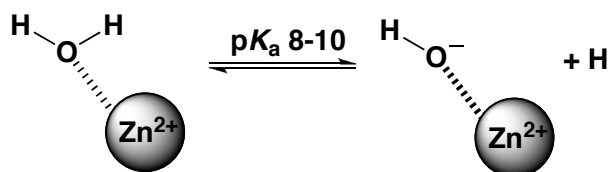
**Figure S2.** The pH dependence of AP for phosphate (A) and tungstate (B) binding. Data are from ref. 4 and affinity values were determined by inhibition of 2-fluoroethyl phosphate hydrolysis (pH 4.5-9.0) and inhibition of *p*NPP hydrolysis (pH 8-11) with  $[S] \ll K_M$ , such that  $K_i$  is expected to be the  $K_d$ . The observed inhibition constants, which were converted to  $K_a$ 's for the plots above, were the same for both substrates at a given pH. For phosphate binding (A), the measurements at low pH are corrected for the amount of covalently bound  $P_i$ . Nonlinear-least-squares fit of the data to a model for two ionizations ( $K_a^{Pi\text{ obs}} = (K_a^{Pi\text{ max}})/(1 + [H^+]/K_1 + K_2/[H^+])$ ) gave  $pK_a$  values of  $5.5 \pm 0.2$  and  $8.2 \pm 0.2$ . The acidic  $pK_a$  does not correspond exactly to the expected  $H_2PO_4^-$   $pK_a$  because further analysis of the pH-dependence not described here suggests an enzymatic group with a  $pK_a$  of  $\sim 5.5$  provides  $\sim 5$ -fold stimulation when protonated (see ref. 4). This enzymatic stimulation offsets the expected acidic limb of  $P_i$  binding by about 1  $pK_a$  unit ( $pK_a$   $H_2PO_4^- \sim 6.6$ ). For tungstate binding (B) the different symbols represent different buffers used and the line represents the best fit of a model for a single ionization at  $pK_a = 8.0 \pm 0.2$ . There is no acidic limb because the tungstate  $pK_a$  is  $< 4.5$ . (Figure adapted from ref. 4)

### Evidence from Prior Studies that the AP Active Site Nucleophile, Ser102, has a $pK_a \leq 5.5$

The pH-dependent  $P_i$  binding studies discussed in the previous section show two limbs, one acidic and one basic, that are log-linear each with a slope of one. The  $pK_a$  associated with the

acidic limb corresponds to the expected  $pK_a$  of the  $P_i$  ligand and for ligands without such a  $pK_a$  there is no pH dependence down to pH 4.5.<sup>4</sup> The  $pK_a$  of the basic limb of any AP pH profile is independent of the ligand  $pK_a$  or even the presence of a titratable group on the ligand, indicating that this limb of the profile is associated with a deprotonation event on the enzyme, as discussed above and in ref. 4.

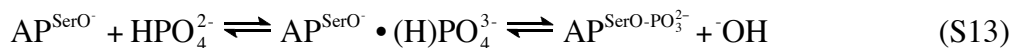
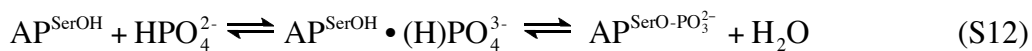
It is possible, in principle, that this deprotonation event at basic pH could be associated with a titration of the AP active site nucleophile, Ser102. This model requires that SerOH (and not SerO<sup>-</sup>) be the active form of the nucleophile and that its  $pK_a$  be 8. This requirement holds despite the greater reactivity of alkoxides than their corresponding alcohols, rendering this model unlikely, although the small values of  $\beta_{\text{NUC}}$  for reactions of phosphate monoesters suggest that the actual difference in reactivity may be modest (for review see ref. 2). In addition, the  $pK_a$  of water, which has a similar  $pK_a$  as alcohols such as serine, is lowered from 16 to 8-10 when coordinated by  $Zn^{2+}$  (Scheme S2);<sup>5</sup> the presence of a  $Zn^{2+}$ -bimetallo site, and possibly the nearby  $Mg^{2+}$  ion in the AP active site (see Scheme 1B main text), would be expected to lower the  $pK_a$  of Ser102 considerably below the range of 8-10. Indeed, pH-dependencies for other  $Zn^{2+}$  bimetallo enzymes are consistent with SerOH  $pK_a$  values  $<6$ ,<sup>6,7</sup> and carbonic anhydrase with only a single  $Zn^{2+}$  ion has a  $pK_a$  of 6.7 for its  $Zn^{2+}$ -coordinated water.<sup>8</sup> Given the above, it is highly unlikely that the  $pK_a$  of 8 that leads to decreased binding and reactivity corresponds to formation of Ser102 alkoxide in AP, with this anion being unable to participate in the enzymatic reaction. As there is no other enzymatic  $pK_a$  from 5.5-11, it is likely that the  $pK_a$  of Ser102 of AP is  $\leq 5.5$ .



**Scheme S2**



The following provides additional evidence for the presence of Ser102 alkoxide across the observed pH profile. To assess whether such a protonation event at Ser102 was responsible for the basic limb of the  $P_i$  binding affinity profile, previous authors considered the pH-dependent equilibrium between the covalent phosphoserine intermediate and noncovalently bound  $P_i$ .<sup>4</sup> Previous pH-dependent  $P_i$  binding results suggest that  $HPO_4^{2-}$  is the species formally bound by the enzyme (see section above). It has also been established by  $^{31}P$ -NMR<sup>9-11</sup> and  $^{32}P$ -labeling studies<sup>12</sup> that AP forms a covalent bond at Ser102 with  $P_i$  at low pH (see main text). Two possible equilibria are shown in eq S12 and S13 depicting the formation of the covalent adduct starting with either protonated or deprotonated Ser102.



Eq S12 predicts that the formation of the covalent AP- $P_i$  species would be pH-independent as no net transfer of protons is involved in the equilibrium. In contrast, eq S13 predicts a pH-dependence as  $^-OH$  is released upon formation of the covalent species. The formation of the AP- $P_i$  covalent species at low pH is pH-dependent, consistent with the equilibrium depicted in eq S13 but not of that depicted in eq S12.<sup>4</sup> This experimental observation provides further evidence against SerOH, with a  $pK_a$  of 8, acting as the active nucleophile.

In summary, the observations and arguments above suggest that neither the acidic nor basic limb observed in the AP• $P_i$  binding affinity pH profile is associated with a titration of Ser102. The acidic limb is accounted for by the ligand  $pK_a$ , and the basic limb is not consistent with a Ser102 titration as suggested by known  $pK_a$  perturbations from  $Zn^{2+}$  and by the covalent adduct formation analysis above. Additional evidence against a Ser102  $pK_a$  corresponding to the basic limb is also discussed further in ref. 4. As the data in the AP• $P_i$  pH binding profile goes

down to pH 4.5 an upper limit for the Ser102  $pK_a$  could be set by this pH. However, the pH profile is complicated by a stimulatory  $pK_a$  at  $\sim 5.5$ ,<sup>4</sup> so we estimate a conservative assignment of the Ser102  $pK_a$  corresponding to the upper limit set by this  $pK_a$  of 5.5.

### **Interpretation of Potential FTIR Signals of AP-phosphoserine at pH 5.0**

As described in the main text, previous <sup>31</sup>P-NMR and biochemical binding studies have indicated that approximately half of AP-bound  $P_i$  at pH 5.0 is bound covalently to Ser102. Thus, it was expected that the FTIR spectrum of AP-bound  $P_i$  at pH 5.0 would reflect equal vibrational contributions from the noncovalently bound  $P_i$  species and the covalently bound phosphoserine monoester.

The first expectation that the pH 5.0 FTIR spectrum should contain peaks associated with noncovalently bound  $P_i$ , was convincingly observed (Figure S3, red arrows). A prominent peak in the pH 5.0 spectrum at  $1015\text{ cm}^{-1}$  has the same frequency and general shape as the peak observed in the pH 8.0 FTIR spectrum, which contains only contributions from noncovalently bound  $P_i$ . In addition, this peak corresponds to the prominent peak observed in the standard  $\text{PO}_4^{3-}$  solution spectrum, suggesting that the noncovalently bound  $P_i$  species in both the pH 8.0 and pH 5.0 samples is  $\text{PO}_4^{3-}$  as discussed in the main text. The corresponding <sup>18</sup>O- $\text{PO}_4^{3-}$  negative peak that was expected at  $972\text{ cm}^{-1}$  based on the pH 8.0 AP and standard solution  $\text{PO}_4^{3-}$  spectra was not as clearly observed in the pH 5.0 spectrum. In the pH 5.0 spectrum this peak is likely masked by the noise that appears at wavenumbers below  $975\text{ cm}^{-1}$  by uncertainties in obtaining a reliable subtracted background. However, there is evidence of a negative peak below  $1000\text{ cm}^{-1}$ , as expected, but this peak appears to be only partially observed due to the background issues.

Additional peaks appear in the pH 5.0 spectrum above 1050  $\text{cm}^{-1}$ . A relatively small positive peak is observed at 1072  $\text{cm}^{-1}$  (Figure S3, green arrow). This peak likely arises from a small population of unbound  $\text{H}_2\text{PO}_4^{1-}$  in the sample because the frequency of the peak most closely corresponds to the positive peak observed at 1077  $\text{cm}^{-1}$  in the standard  $\text{P}_i^{1-}$  solution spectrum. The corresponding negative peak for this species in the pH 5.0 AP spectrum (expected around 1038  $\text{cm}^{-1}$ ) is masked by the more intense 1015  $\text{cm}^{-1}$  peak.

The other peaks observed in the pH 5.0 spectrum are more difficult to interpret because the frequencies of these peaks do not correspond to any of the  $\text{P}_i$  solution spectra. Based on the second expectation at pH 5.0, that approximately half of the  $\text{P}_i$  is bound covalently, we suggest that these peaks may correspond to the vibrational properties of the phosphoserine monoester. For alkyl phosphate monoester model compounds, observed IR frequencies fall within the 1089-1110  $\text{cm}^{-1}$  range (for the asymmetric stretching frequency).<sup>13</sup> In our pH 5.0 spectrum there is a pair of prominent peaks within this range (negative peak, 1089  $\text{cm}^{-1}$ ; positive peak, 1107  $\text{cm}^{-1}$ ; black arrows in Figure S3). This peak pair presumably arises from the phosphoserine covalent species.

Interestingly, the wavenumber difference between this peak pair is smaller (18  $\text{cm}^{-1}$ ) than expected for a  $^{16}\text{O}/^{18}\text{O}$ -labeled phosphate group based on the wavenumber differences observed for peak pair frequencies of  $\text{P}_i$  and other phosphate monoesters (25-45  $\text{cm}^{-1}$  shifts typically observed for these compounds upon  $^{18}\text{O}$ -labeling). One explanation for the unusual peak pair difference observed is that the vibrational properties of the AP phosphoserine are perturbed by influences from the active site relative to the expected vibrational properties from a solution version of the phosphoserine monoester. This explanation is consistent with previous interpretations of the AP phosphoserine  $^{31}\text{P}$ -NMR chemical shift; the chemical shift of the AP

phosphoserine species is shifted downfield by  $\sim 6$  ppm from the expected chemical shift of the small molecule phosphoserine.<sup>9</sup> This proposed perturbation may also influence the vibrational properties of covalently bound phosphate resulting in the unexpected peak pair frequency differences observed in our pH 5.0 FTIR spectrum. Also, changes in the  $\text{Zn}^{2+}$ - $\text{P}_i$  interactions in the covalent complex relative to the noncovalent complex could result in vibrational mode decoupling since only one or two of the P-O bonds in  $\text{P}_i$  interact with the  $\text{Zn}^{2+}$  ions. Such a change in interaction energy could break the vibrational symmetry of the bound  $\text{P}_i$  molecule resulting in peak splitting or pattern changes to the AP-bound phosphoserine spectrum. These and other possibilities make it difficult to directly assign peaks to the phosphoserine AP covalent species. But in the absence of further tests, we adopt the most likely explanation that the 1089 and 1107  $\text{cm}^{-1}$  peaks correspond to the covalently bound  $\text{P}_i$  species expected at pH 5.0.

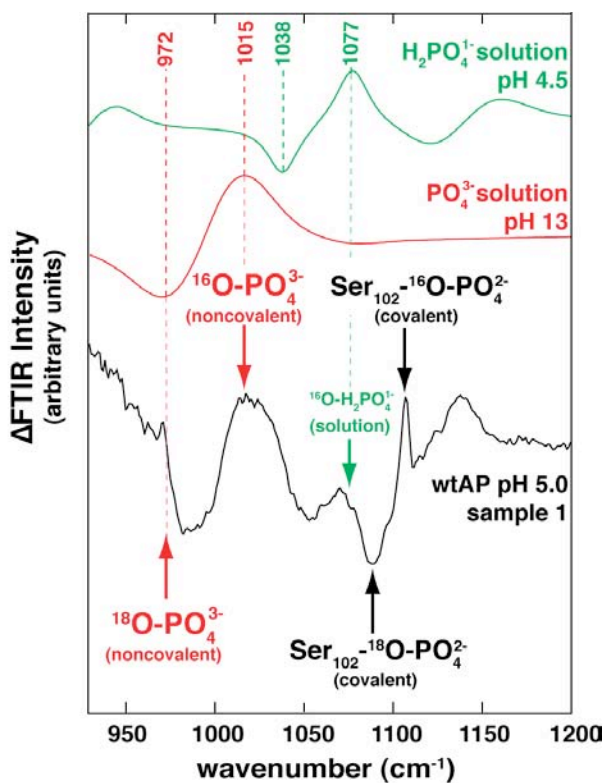


**Figure S3.** [ $^{18}\text{O}$ ]- $\text{P}_i$  edited FTIR difference spectra of  $\text{P}_i$  in solution and AP-bound at pH 5.0. FTIR difference spectrum between  $^{16}\text{O}$ - $\text{P}_i$  and  $^{18}\text{O}$ - $\text{P}_i$  at pH 4.5 (green) or pH 13 (red). FTIR

difference spectrum between AP•<sup>16</sup>O-P<sub>i</sub> and AP•<sup>18</sup>O-P<sub>i</sub> (4.6 mM AP, 2.8 mM P<sub>i</sub>) in 10 mM NaAcetate, pH 5.0, 100 mM NaCl, 100 μM ZnCl<sub>2</sub>, and 1 mM MgCl<sub>2</sub> (Sample 1, black). Red arrows mark the expected peak frequencies for noncovalently bound PO<sub>4</sub><sup>3-</sup> corresponding to the PO<sub>4</sub><sup>3-</sup> solution spectrum. The green arrow indicates the expected positive peak frequency for H<sub>2</sub>PO<sub>4</sub><sup>1-</sup> from the standard H<sub>2</sub>PO<sub>4</sub><sup>1-</sup> solution spectrum above. This relatively small peak likely arises from an unbound population of H<sub>2</sub>PO<sub>4</sub><sup>1-</sup>. The black arrows indicate the positive and negative peaks proposed to arise from the AP phosphoserine covalent species. The unmarked positive peak at 1138 cm<sup>-1</sup> is unidentified and may also arise from a relatively small contribution of unbound H<sub>2</sub>PO<sub>4</sub><sup>1-</sup> although the correspondence to the H<sub>2</sub>PO<sub>4</sub><sup>1-</sup> solution spectrum is less than expected.

### **Analysis for Potential Coincidental Shifts of Observed FTIR Spectra**

The observed AP with P<sub>i</sub> FTIR pH 8.0 difference spectrum could coincidentally reflect HPO<sub>4</sub><sup>2-</sup> with shifted vibrational properties if the peak pair observed at 1015 and 972 cm<sup>-1</sup> actually correspond to the peak pair associated with the asymmetric stretching frequencies at 1081 and 1044 cm<sup>-1</sup> of the solution HPO<sub>4</sub><sup>2-</sup> (Figure S4). For the observed peak pair to correspond to the HPO<sub>4</sub><sup>2-</sup> asymmetric peak pair, a shift of -66 cm<sup>-1</sup> upon binding would be required (Figure S4A). A shift this large to the solution vibrational frequencies of the P<sub>i</sub> ligand upon protein binding would be unprecedented<sup>14-16</sup>. Furthermore, we do not expect the observed peak pair to correspond to the asymmetric solution HPO<sub>4</sub><sup>2-</sup> peaks based on the difference between the frequencies of the positive and negative peak pair. The frequency difference between the positive and negative peaks of the HPO<sub>4</sub><sup>2-</sup> solution spectrum is 37 cm<sup>-1</sup> while the difference between the observed peaks is 43 cm<sup>-1</sup>. Therefore, the difference between the positive and negative peaks of the observed spectrum does not agree with the peak difference of the asymmetric vibrational frequencies of the solution HPO<sub>4</sub><sup>2-</sup>. This difference further suggests that the observed AP with P<sub>i</sub> spectrum does not represent the asymmetric stretching frequencies for HPO<sub>4</sub><sup>2-</sup>.

We also considered the opposite coincidental frequency shift that would result in the observed peaks corresponding to the symmetric stretching frequencies of the solution  $\text{HPO}_4^{2-}$  (Figure 4B). If the symmetric peak frequencies of the  $\text{HPO}_4^{2-}$  ligand at 947 and 990  $\text{cm}^{-1}$  shifted by +25  $\text{cm}^{-1}$  upon binding, then the observed peaks in the AP sample would correspond to the symmetric stretching frequencies of bound  $\text{HPO}_4^{2-}$ . This frequency shift would not be unprecedented; however, given the observation window of the measurement, we would then also expect to observe the correspondingly shifted asymmetric peaks of the  $\text{HPO}_4^{2-}$  at 1106 and 1069  $\text{cm}^{-1}$ , assuming that the protein induced frequency shifts effect both symmetric and asymmetric stretching frequencies equally. We do not observe an additional set of peaks in this frequency range, again suggesting that the observed spectrum does not reflect  $\text{HPO}_4^{2-}$  with shifted vibrational properties.

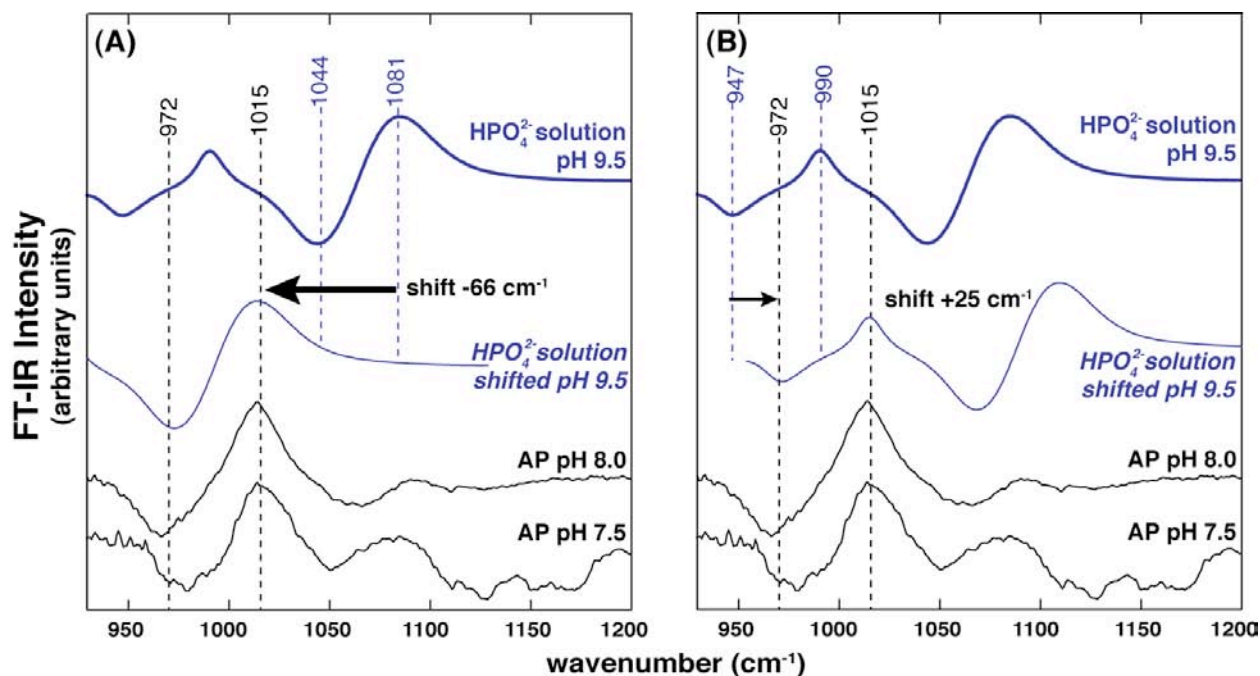


**Figure S4.** A comparison of the  $\text{HPO}_4^{2-}$  solution spectrum and the hypothetical shifts of this spectrum that would be required to resemble the observed  $\text{P}_i$ -bound AP spectra. (A) If the peaks at 1015 and 972  $\text{cm}^{-1}$  in the observed spectra reflect the  $\text{HPO}_4^{2-}$  asymmetric peak pair, an unprecedented shift to the solution-like asymmetric vibrational frequency of  $\text{HPO}_4^{2-}$  of 66  $\text{cm}^{-1}$

would be required upon AP-binding. Note that the difference between the asymmetric peak pair of  $\text{HPO}_4^{2-}$  (at 1081 and 1044  $\text{cm}^{-1}$ ) is larger than the difference between the peaks in the observed  $\text{P}_i$ -bound AP spectra. (B) If the observed peaks in the  $\text{P}_i$ -bound AP spectra reflect the  $\text{HPO}_4^{2-}$  symmetric peak pair at 990 and 947  $\text{cm}^{-1}$  a shift to the solution-like vibrational frequency of  $\text{HPO}_4^{2-}$  of 25  $\text{cm}^{-1}$  would be required. Note, however, that this shift also leaves the asymmetric peak pair within the observation window. This peak pair is not observed in the  $\text{P}_i$ -bound AP spectra.

### **Determination of $\text{PO}_4^{3-}$ Affinity for Deprotonated Ser102 AP**

The  $\text{PO}_4^{3-}$  affinity for deprotonated Ser102 AP can be estimated by measuring the  $\text{P}_i$  affinity across a pH range. In principle, the observed  $\text{P}_i$  binding at a given pH can reflect the binding contributions of any of the  $\text{P}_i$  species. The results presented in the main text indicate that the observed  $\text{P}_i$  affinity in the neutral pH range reflects the binding of  $\text{HPO}_4^{2-}$  specifically (resulting in an internal proton transfer presumably to Ser102 and the formation of bound  $\text{PO}_4^{3-}$ ). The contribution of  $\text{HPO}_4^{2-}$  binding to the overall observed  $\text{P}_i$  binding is expected to be constant at pH values well below the  $\text{HPO}_4^{2-}$   $\text{p}K_a$  (11.7) as the proportion of  $\text{HPO}_4^{2-}$  in solution remains nearly constant up to pH values approaching the  $\text{p}K_a$ . However, as the pH approaches the  $\text{HPO}_4^{2-}$   $\text{p}K_a$  and the proportion of  $\text{PO}_4^{3-}$  in solution increases, the overall observed  $\text{P}_i$  affinity could start to reflect a binding contribution from  $\text{PO}_4^{3-}$ . Any influence of  $\text{PO}_4^{3-}$  on the observed  $\text{P}_i$  affinity will depend on the solution pH and the  $\text{PO}_4^{3-}$  affinity relative to the apparent  $\text{HPO}_4^{2-}$  affinity. An increase in the observed  $\text{P}_i$  affinity as the pH is raised would indicate a binding contribution from  $\text{PO}_4^{3-}$ . As all of the Ser102 AP will be deprotonated at these pH values ( $\text{p}K_a \leq 5.5$ ),  $\text{PO}_4^{3-}$  binding that increases as pH increases would be to deprotonated Ser102 AP.

The observed pH-dependent  $\text{P}_i$  binding to AP is complicated by an inactivating  $\text{p}K_a$  of  $\sim 8.2$  associated with free AP.<sup>4</sup> Nevertheless, this inactivating titration can be accounted for and if  $\text{PO}_4^{3-}$  makes a binding contribution at higher pH values, we still expect to see an upward trend

from the observed affinity. To ensure that AP remains functional even at very high pH values, we plotted the *p*-nitrophenyl phosphate (*p*NPP) hydrolysis activity throughout the pH range. Reactions were measured to completion under conditions in which  $[S] < K_M$  as described previously.<sup>4,17</sup> As *p*NPP has no titratable protons in this pH range we expected to observe a continuous log linear decrease in activity reflecting only the  $pK_a$  associated with AP. Negative deviations from this trend would have indicated unpredictable loss of enzyme activity (potentially due to unfolding). We observed a simply behaved pH-dependence of *p*NPP activity out to pH 11.4 (Figure S5A) that could be fit to eq S14 for two rate-controlling ionizations (also as reported previously to pH 11, ref. 17). Loss of activity was observed at  $pH > 11.4$  and thus, we only carried out the  $P_i$  affinity measurements to this pH.

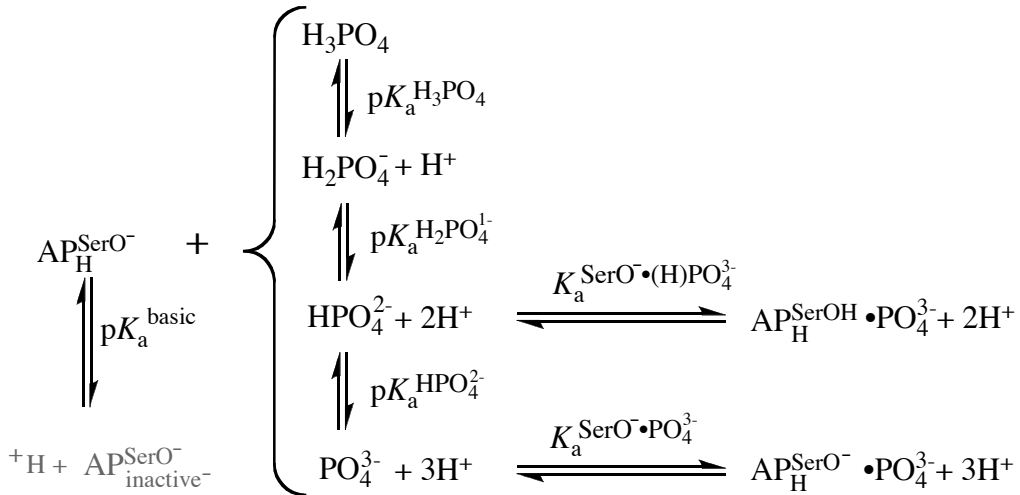
$$(k_{\text{cat}}/K_M)^{\text{obs}} = \frac{(k_{\text{cat}}/K_M)^{\text{max}}}{\left(1 + 10^{pK_a^{\text{acidic}} - \text{pH}} + 10^{\text{pH} - pK_a^{\text{basic}}}\right)} \quad (\text{S14})$$

The  $P_i$  affinity data from pH 7.0-11.4 is shown in Figure S5B. The  $P_i$  affinity data shows no significant deviation from the expected  $\text{HPO}_4^{2-}$  affinity trend even up to pH 11.4 where the proportion of  $\text{PO}_4^{3-}$  in solution is above 10%. Because no influence of  $\text{PO}_4^{3-}$  binding was detected we could only set a lower limit for the dissociation constant of  $\text{PO}_4^{3-}$  binding to deprotonated Ser102 AP ( $K_a^{\text{SerO}^- \cdot \text{PO}_4^{3-}}$ ). To estimate the lower limit, eq S15, derived from Scheme S3, was used to fit the data from pH 7.0-11.0. The  $\text{PO}_4^{3-}$  affinity in eq S15 was fixed at a series of values corresponding to decreasing  $K_a^{\text{SerO}^- \cdot \text{PO}_4^{3-}}$  values as shown in Figure S5B. The observed deviations of the fits to the data at pH 11.0-11.4 (open circles) were used to set a lower limit for the  $\text{PO}_4^{3-}$  affinity. Clear deviations from the high pH data are observed if  $K_a^{\text{SerO}^- \cdot \text{PO}_4^{3-}}$  is set to values lower



than 100 nM. Thus, the  $\text{PO}_4^{3-}$  disassociation constant for deprotonated Ser102 AP must be greater than 100 nM.

$$K_a^{\text{P}_i^{\text{observed}}} = \left( \frac{1}{1 + 10^{\text{pH} - \text{p}K_a^{\text{basic}}}} \right) \times \left( \frac{K_a^{\text{SerO}^- \cdot (\text{H})\text{PO}_4^{3-}}}{\left( 1 + 10^{\text{p}K_a^{\text{H}_3\text{PO}_4} + \text{p}K_a^{\text{H}_2\text{PO}_4^{1-}} - 2\text{pH}} + 10^{\text{p}K_a^{\text{H}_2\text{PO}_4^{1-}} - \text{pH}} + 10^{\text{pH} - \text{p}K_a^{\text{HPO}_4^{2-}}} \right) + \frac{K_a^{\text{SerO}^- \cdot \text{PO}_4^{3-}}}{\left( 1 + 10^{\text{p}K_a^{\text{HPO}_4^{2-}} + \text{p}K_a^{\text{H}_2\text{PO}_4^{1-}} + \text{p}K_a^{\text{H}_3\text{PO}_4} - 3\text{pH}} + 10^{\text{p}K_a^{\text{HPO}_4^{2-}} + \text{p}K_a^{\text{H}_2\text{PO}_4^{1-}} - 2\text{pH}} + 10^{\text{p}K_a^{\text{HPO}_4^{2-}} - \text{pH}}} \right)} \right) \quad (\text{S15})$$



**Scheme S3**

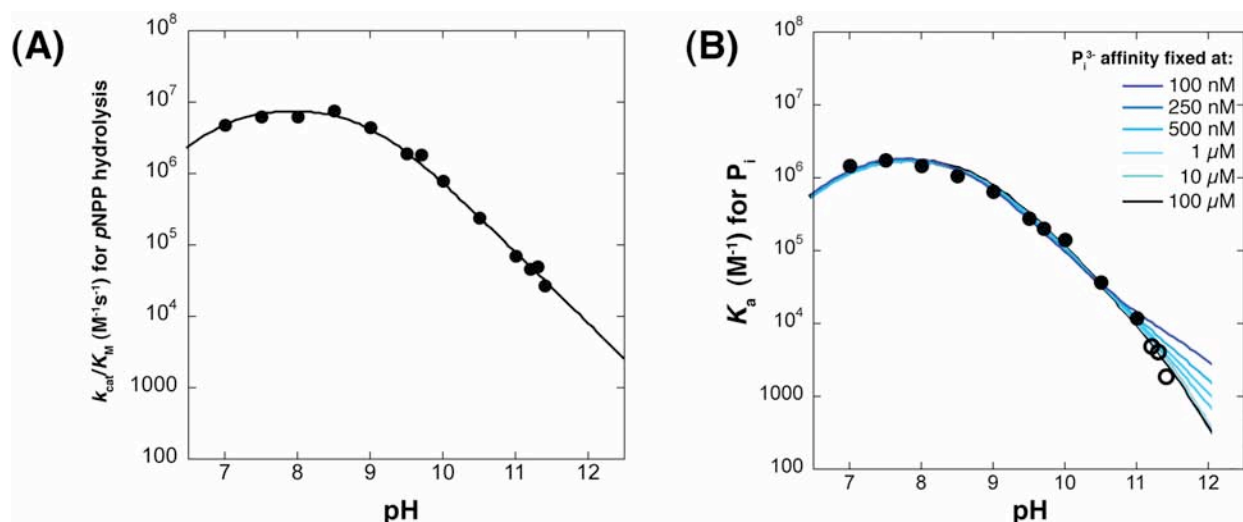


**Figure S5.** Analysis for  $\text{PO}_4^{3-}$  binding affinity for deprotonated Ser102 AP. The size of the data points corresponds to the estimated error of 20% (A) The pH-dependent *p*NPP hydrolysis activity of AP behaves predictably out to pH 11.4. Standard reaction assay conditions of 100 mM NaAcetate (pH 4.5-5.5), NaMaleic Acid (pH 6.0-6.5), NaMOPS (pH 7-8.0), NaCHES (pH 8.5-9.5), NaCAPS (pH 10-11.2), NaCABS (pH 11.0-11.4), 100 mM NaCl, 1 mM  $\text{MgCl}_2$ , and 100  $\mu\text{M}$   $\text{ZnCl}_2$  were used at 25 °C. A non-linear least squares fit (Kaleidagraph, Synergy Software) of eq S14 yielded a fit with  $\text{p}K_a^{\text{acidic}} = 6.9$ ,  $\text{p}K_a^{\text{basic}} = 8.9$  and a  $(k_{\text{cat}}/K_M)^{\text{max}} = 8.6 \times 10^6 \text{ M}^{-1}\text{s}^{-1}$  in reasonable agreement with previous results.<sup>17</sup> (B) The pH-dependent  $\text{P}_i$  affinity of AP observed to pH 11.4 under the standard assay conditions above. The data from pH 7.0-11.0 (solid circles) were fit using a non-linear least squares fit of eq S15 at various fixed values of  $K_a^{\text{SerO}^- \cdot \text{PO}_4^{3-}}$  corresponding to the  $K_d^{\text{SerO}^- \cdot \text{PO}_4^{3-}}$  values shown. All fits gave  $K_d^{\text{SerO}^- \cdot (\text{H})\text{PO}_4^{3-}}$  values of  $\sim 0.5 \mu\text{M}$  and  $\text{p}K_a^{\text{basic}} \sim 8.7$ . The fit using a fixed  $K_d^{\text{SerO}^- \cdot \text{PO}_4^{3-}}$  of 100 nM deviated 4-fold from the data from pH 11.0-11.4 (open circles) - a larger deviation than expected from the estimated error of these measurements (<50%).

### Description of ground state destabilization via restriction in conformational freedom

As noted in the main text, interactions that increase the energy of the  $\text{E} \cdot \text{S}$  state relative to the  $\text{E} + \text{S}$  and transition states are defined as ground state destabilizing (Figure 5C main text)<sup>18-20</sup>, and the most common origin of ground state destabilization is likely a conformational entropy penalty arising from the binding and positioning of substrates in a restricted set of conformations such that the substrates are next to each other and next to reactive groups in the active site. This effect is easiest to appreciate for a bi-molecular reaction in which two substrates,  $\text{S}_1$  and  $\text{S}_2$ , must come together to react (as depicted in Figure S6 for corresponding enzymatic and nonenzymatic

reactions). In both the nonenzymatic reaction and the enzymatic reaction starting from the free substrates and free enzyme there is a penalty in conformational entropy for positioning the reactants together in the transition state, formally resulting in the loss of several degrees of translational and rotational degrees of freedom for each reactant.<sup>1</sup>

We extend an analogy used by Jencks in terms of ‘paying’ the energetic price for a reaction.<sup>18</sup> Our enzyme is akin to a special VIP card that can be purchased upon entry to an amusement park that allows you to skip the long lines.<sup>24</sup> With this card, a barrier for entering a ride is removed since we pay less in waiting time for each ride once in the amusement park; with the enzyme we ‘pay’ less in energy to reach the transition state because a reaction barrier of conformational entropy has been removed or lessened. In other words, by forming the  $E \cdot S_1 \cdot S_2$  ground state, the loss in conformational entropy that must occur to accomplish the reaction is already paid for – it is paid for by the binding interactions that position the two substrates with respect to one another; in contrast, in the nonenzymatic reaction this entropic penalty must still be paid in the progression from the  $S_1 + S_2$  free state to the  $S_1 \cdot S_2^\ddagger$  transition state ( $\Delta S_{\text{solution}}^\ddagger$  in Figure S6). Thus, the entropic component of the barrier for the nonenzymatic reaction is larger.<sup>2</sup> The enzyme-bound ground state is destabilized relative to a hypothetical enzyme that makes the same interactions with the substrates but accomplishes less restriction of motion of the substrates with

---

<sup>1</sup> Unfortunately, what we consider conceptually as ‘entropy’ is typically the freedom of motion of reactants, whereas experimental measures of  $\Delta S$  includes all of the species present and, in practice, are often dominated by contributions from the surroundings –solvent molecules and/or the enzyme. Deconvolution of these contributions is an unmet challenge, although there is interesting work in this area.<sup>21-23</sup>

<sup>2</sup> In the amusement park, with your VIP card you are positioned at the start of the ride, whereas those who cannot afford the card have to start at the back of the line and experience a longer path – or larger conformational barrier – to get to the ride.

respect to one another.<sup>3</sup> Thus, the enzyme selectively destabilizes the ground state, as depicted in Figure 5C in the main text. The same arguments can be made for single substrate reactions for which binding positions the substrate with respect to catalytic groups on the enzyme, analogous to positioning substrates with respect to one another as described above.

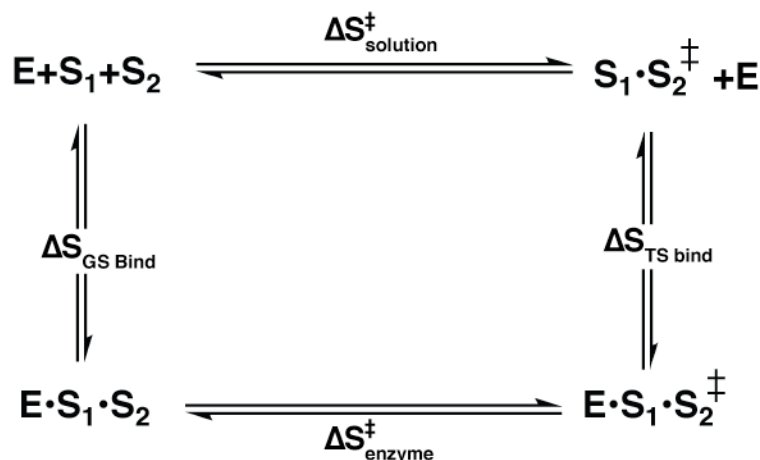


**Figure S6.** Thermodynamic cycle illustrating considerations of conformational entropy for enzyme-catalyzed and solution reactions. As noted in the main text, we use the terms entropy and conformational entropy here to refer to the degree of restriction in freedom of motion of the substrates with respect to one another, although these properties cannot yet be parsed experimentally. The entropic penalty for the solution reaction ( $\Delta S_{\text{solution}}^\ddagger$ ) is larger than the entropic penalty for the enzymatic reaction ( $\Delta S_{\text{enzyme}}^\ddagger$ ) because binding energy is used to offset the conformational entropy cost ( $\Delta S_{\text{enzyme}}^\ddagger < \Delta S_{\text{solution}}^\ddagger$ ). Utilization of binding energy to align substrates for reaction results in an apparent destabilization of the enzyme ground state relative to a hypothetical enzyme that provides less conformational restriction of its substrates but maintains the same binding interactions and thus achieves stronger binding. For an ideal case in which the enzyme precisely positions the reactants, there would be little or no additional conformational restrictions upon forming  $E \cdot S_1 \cdot S_2^\ddagger$  from  $E \cdot S_1 \cdot S_2$  ( $\Delta S_{\text{enzyme}}^\ddagger$  negligible). Independent motion is restricted in the  $S_1 \cdot S_2^\ddagger$  nonenzymatic transition state by definition, due to formation of a partial covalent bond between the substrates. Thus, less conformational entropy is lost upon association of the transition state with the enzyme than upon association of the two substrates with the enzyme ( $\Delta S_{\text{TS Bind}} < \Delta S_{\text{GS Bind}}$ ).

<sup>3</sup> Many of the comparisons made in describing energetic concepts are crude approximations of physical behavior but are nevertheless useful as idealized examples that allow us to better understand the underlying energetic concepts. Indeed, we are still unable to fully describe the conformational states and energetics of enzymatic reactions; this remains a major challenge.

## Supporting References

- (1) Lad, C.; Williams, N. H.; Wolfenden, R. *Proc. Natl. Acad. Sci. U.S.A.* **2003**, *100*, 5607-5610.
- (2) Lassila, J. K.; Zalatan, J. G.; Herschlag, D. *Annu. Rev. Biochem.* **2011**, *80*, 669-702.
- (3) Martell, A. E.; Smith, R. M. *Critical Stability Constants, Vol. 1-6* **1989**, Plenum Press, New York.
- (4) O'Brien, P. J.; Herschlag, D. *Biochemistry* **2002**, *41*, 3207-3225.
- (5) Jencks, W. P.; Regenstein, J. In *Handbook of Biochemistry and Molecular Biology*; Fasman, G. D., Ed.; CRC: Cleveland, OH, 1976.
- (6) Bounaga, S.; Laws, A. P.; Galleni, M.; Page, M. I. *Biochem J.* **1998**, *331*, 703-711.
- (7) Mock, W. L.; Tsay, J. T. *J. Biol. Chem.* **1988**, *263*, 8635-8641.
- (8) Pocker, Y.; Bjorkquist, D. W. *Biochemistry* **1977**, *16*, 5698-5707.
- (9) Chlebowski, J.; Armitage, I.; Tusa, P.; Coleman, J. *J. Biol. Chem.* **1976**, *251*, 1207-1261.
- (10) Gettins, P.; Coleman, J. E. *J. Biol. Chem.* **1983**, *258*, 408-416.
- (11) Chlebowski, J. F.; Armitage, I. M.; Coleman, J. E. *J. Biol. Chem.* **1977**, *252*, 7053-7061.
- (12) Schwartz, J. H. *Proc. Natl. Acad. Sci. U.S.A.* **1963**, *49*, 871-878.
- (13) Cheng, H.; Nikolic-Hughes, I.; Wang, J. H.; Deng, H.; O'Brien, P. J.; Wu, L.; Zhang, Z.-Y.; Herschlag, D.; Callender, R. *J. Am. Chem. Soc.* **2002**, *124*, 11295-11306.
- (14) Wang, J. H.; Xiao, D. G.; Deng, H.; Webb, M. R.; Callender, R. *Biochemistry* **1998**, *37*, 11106-11116.
- (15) Cheng, H.; Sukal, S.; Deng, H.; Leyh, T.; Callender, R. *Biochemistry* **2001**, *40*, 4035-4043.
- (16) Deng, H.; Lewandowicz, A.; Schramm, V. L.; Callender, R. *J. Am. Chem. Soc.* **2004**, *126*, 9516-9517.
- (17) O'Brien, P. J.; Herschlag, D. *J. Am. Chem. Soc.* **1998**.
- (18) Jencks, W. P. *Advances in Enzymology* **1975**, *43*, 219-410.
- (19) Jencks, W. P. *Cold Spring Harb. Symp. Quant. Biol.* **1987**, *52*, 65-73.
- (20) Murphy, D. *Biochemistry* **1995**, *34*, 4507-4510.
- (21) Kraut, D. A.; Carroll, K. S.; Herschlag, D. *Annu. Rev. Biochem.* **2003**, *72*, 517-571.
- (22) Frederick, K. K.; Marlow, M. S.; Valentine, K. G.; Wand, A. J. *Nature* **2007**, *448*, 325-329.
- (23) Marlow, M. S.; Dogan, J.; Frederick, K. K.; Valentine, K. G.; Wand, A. J. *Nat. Chem. Biol.* **2010**, *6*, 352-358.
- (24) Mohny, C. *Slate Online Magazine* **2002**, <http://www.slate.com/id/2067672/>.